Time of Flight system Design study

Rajendran Raja
7 Sep-02

Preamble

We consider a time of flight array of dimensions hdx,hdy,hdz = (230.0,120.0,2.5) cm, where hdx,hdy and hdz are the ***half*** lengths in x,y and z. The direction x is horizontal., y vertical and z is the beam direction. Each scintillator has hdx=2,5 cm. There are 92 counters in all in this array. The radiation length of scintillator in Geant is 42.2 cm and the interaction length is 88.7 cm. 5cm of scintillator in the beam direction is equivalent to 0.118 radiation lengths and 0.056 interaction lengths. The midpoint of the array is placed at –283.699 cm in z in the mother volume, the target being at –832.55cm and the center of the Jolly Green Giant being at –739.998 cm. The distance from the target to the center of the ToF system is 548.851 cm. The time taken by light to travel this distance is 18.307 ns. An accuracy of 150 ps in ToF measurement is thus a 0.819% measurement of the ToF.

Figure 1 shows the total radiation lengths as a function of z as seen by an infinite momentum beam particle on the beam axis in MIPP. Figure 2 shows the total number of interaction lengths as a function of z. The total number of radiation lengths just after the ToF is 0.343. i.e a 5cm thick ToF contributes 50% additional to all that preceded it in radiation lengths. The total number of interaction lengths just after the ToF is 0.109. The ToF contributes 105% additional interaction lengths to all that preceded it.

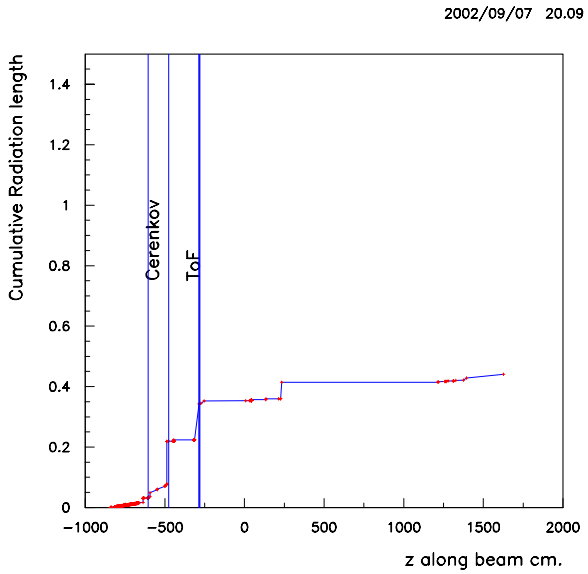

Figure 1 Cumulative Radiation Length vs distance along beam

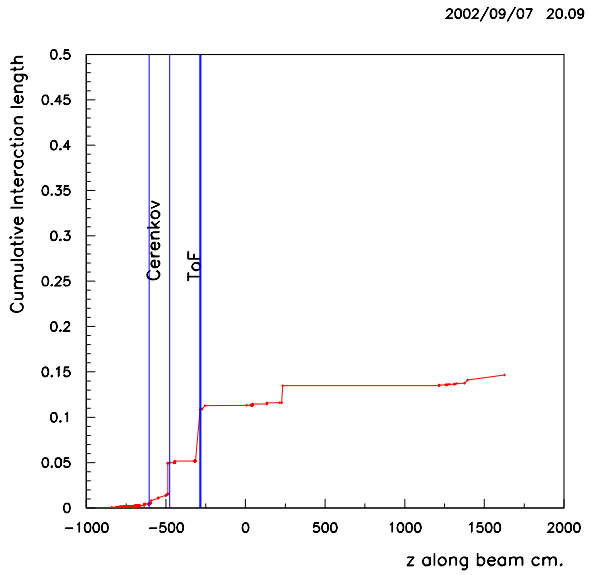

Figure 2 Cumulative Interaction length vs distance along beam

Error analysis

The momentum p of the particle is related to its rest mass by the formula $p = m_0 \gamma \beta c$. Differentiating this leads to $\frac{\partial m_0}{m_0} = \frac{\partial p}{p} - \gamma^2 \frac{\partial \beta}{\beta}$. Since β is measured by measuring the time t taken to travel the length L, i.e. $\beta = \frac{L}{ct}$, this leads to $\frac{\partial m_0}{m_0} = \frac{\partial p}{p} - \gamma^2 (\frac{\partial L}{L} - \frac{\partial t}{t})$. These individual terms add in quadrature to give the percentage error in mass

$$\left(\frac{\partial m_0}{m_0}\right)^2 = \left(\frac{\partial p}{p}\right)^2 + \gamma^4 \left(\left(\frac{\partial L}{L}\right)^2 + \left(\frac{\partial t}{t}\right)^2 \right)$$

If we measure t to 150ps accuracy, we have seen that this corresponds to a fractional error of 0.8% in t. What is the fractional error in L and p?

To estimate the fractional error in L, we assume an infinite momentum trajectory (straight line) that leaves the vertex and strikes the ToF array. Let x,y,z denote the difference in the Cartesian co-ordinates of the vertex and the point of impact of the trajectory at the ToF.

Then $L^2 = x^2 + y^2 + z^2$ and

.

$$\frac{\partial L}{L} = \frac{x \partial x}{L^2} + \frac{y \partial y}{L^2} = \frac{x \partial x}{L^2} + \frac{y \partial \theta}{z}$$

where θ is the angle the track makes to the z axis in the zy plane.
If we assume, very pessimistically, that the best precision in the x point of impact is the x width of the array element/sqrt(12)=1.44cm, then for the maximum value of x=230cm, the contribution to δL/L from the x co-ordinate is 0.00106. The precision in the angle measurement in y is given by the TPC measurement. If we measure one point in the TPC on the track at the nominal precision of 200 microns over a lever arm of 250cm, then the contribution to δL/L from the y co-ordinate is 1.72E-5 at the maximum value of y=120cm. With proper tracking, we can do better than these pessimistic estimates, especially in x. But even with these pessimistic estimates, the error from δL/L can be neglected as compared to δt/t. So henceforth we write

$$\left(\frac{\partial m_0}{m_0}\right)^2 = \left(\frac{\partial p}{p}\right)^2 + \gamma^4\left(\frac{\partial t}{t}\right)^2$$

We will proceed to estimate δp/p. Before we do this, let us assume that it is negligible and compute the error bands around the masses from δt/t alone.

Some kinematical distributions

Figure 3 shows the variation of γ^2 as a function of momentum for π,K and p. It can be seen that the pion γ^2 is an order of magnitude greater than the kaon at a momentum of 2GeV/c. This feeds directly into the error in the mass determination.

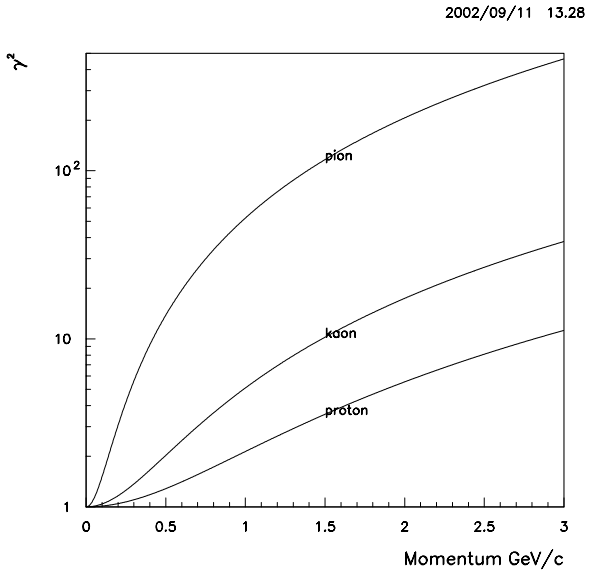

Figure 3 γ^2 as a function of momentum for the three particle types

Figure 4 shows the resulting error in mass, assuming an error of 150ps for the time for the three particle types.

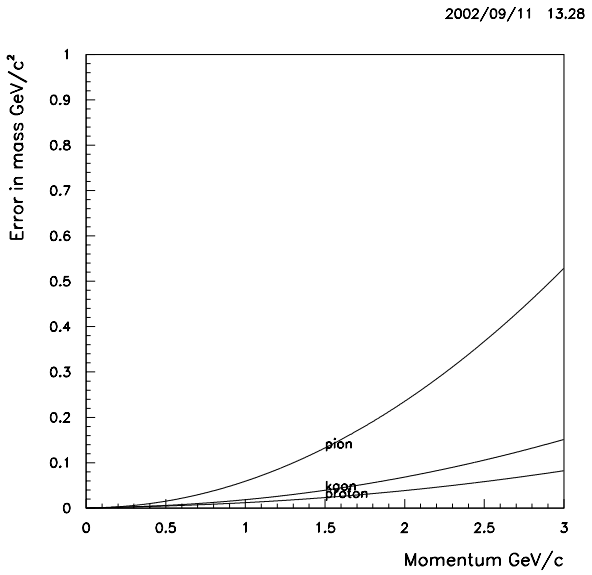

Figure 4 Error in the mass as a function of momentum

We can now map out the mass momentum plane with particle identification, with the assignment of the maximum(Gaussian) likelihood mass as the particle id. Figure 5 results, with red connoting pion, cyan Kaon and yellow proton hypotheses. The island of pion hypothesis in between the K/p masses, as well as above the proton mass results from the pion hypothesis being more likely in these areas due to larger errors in mass resulting from the larger γ^2 for the pion.

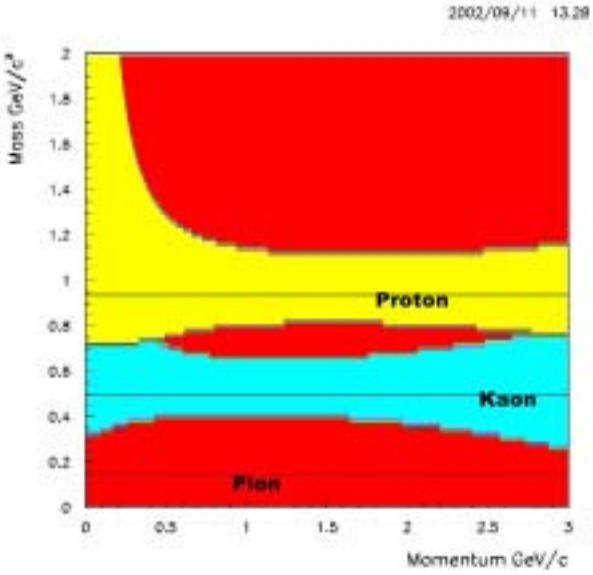

Figure 5 Mass hypothesis assignment contours. Red denotes pion, cyan denotes Kaon and yellow denotes proton. Horizontal lines are the nominal π,K p masses. Gaussian distributions in mass assumed

Since we are working with time measurements with errors, it is possible to get particles with faster than light velocities, $\beta>1$. For these ``tachyons", γ^2 will be negative and m_0^2 will be negative. So rather than work with mass m_0, we choose to analyze in m_0^2. Then

$$\frac{\partial m_0^2}{m_0^2} = 2\frac{\partial m_0}{m_0}$$

This results in Figure 6, which shows the error in m_0^2 as a function of momentum.

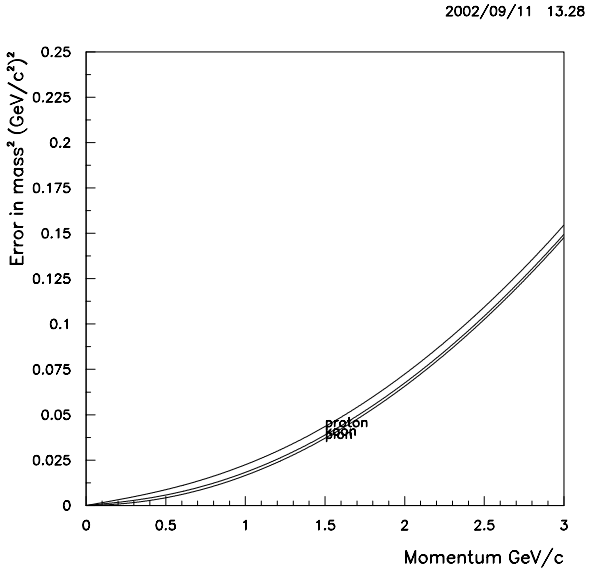

Figure 6 Error in m_0^2 as a function of momentum.

The reason the three particle types follow nearly the same curve in this variable is because the error in m_0^2 is proportional to the energy^2 of the particle. If we assume that the likelihoods are Gaussian in mass^2, then the separation plot as shown in Figure 7 results. Figure 5 and Figure 7 are different, since the distribution can be Gaussian in either mass or mass^2 but not both! In what follows, we will assume that it is Gaussian in mass^2. This permits negative values of mass^2. We can now compute the number of standard deviations the equal likelihood contours are from the respective mass hypotheses as a function of momentum. This is shown in Figure 8. The pion is 3σ away from the Kaon band at a momentum of ~ 1.5 GeV/c where as a Kaon is 3s away from a proton hypothesis at a momentum of ~ 2.5 GeV/c. Since the errors for π,K and p are nearly equal as a function of momentum (Figure 6), the number of standard deviations for π/K, K/p and π/p are very nearly the same as those for K/π p/K and p/π respectively.

Monte Carlo Results

We will now use events from E907 Monte Carlo to study the ToF system further. Figure 9 shows the momentum spectrum of all tracks below 3 GeV/c, all charged tracks and all the charged tracks intercepted by our ToF array. 1000 pp events at 120 GeV/c incoming beam momentum were generated by Pythia for this purpose. Pythia generates a significant number of photons during its string fragmentation process. Figure 10 shows

the acceptance of the ToF as a function of momentum. It can be seen that the acceptance reaches 80% as the momentum goes to 3 GeV/c.

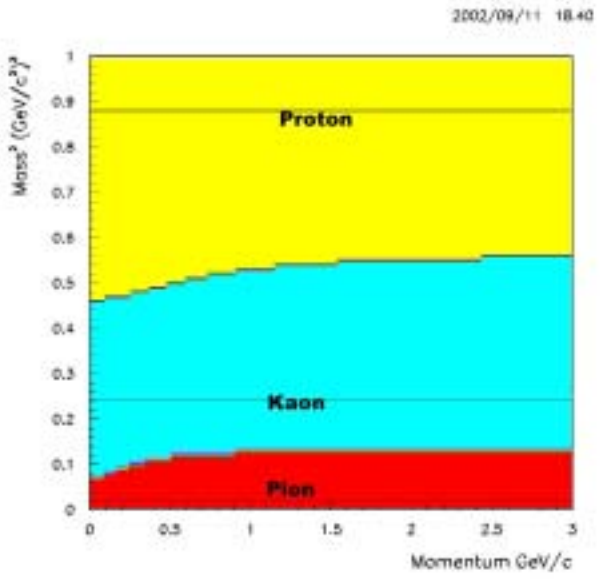

Figure 7 Mass hypothesis assignment contours. Red denotes pion, cyan denotes Kaon and yellow denotes proton. Horizontal lines are the nominal π,K p masses. Gaussian distributions in mass^2 assumed

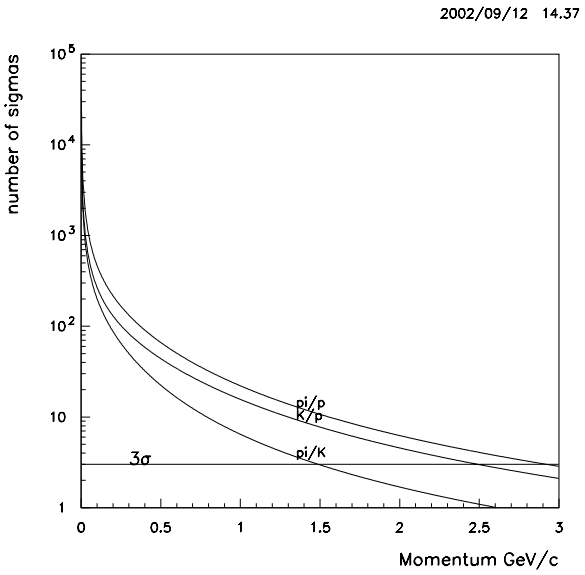

Figure 8 Number of σ's the equal likelihood contours are away from the mass hypotheses

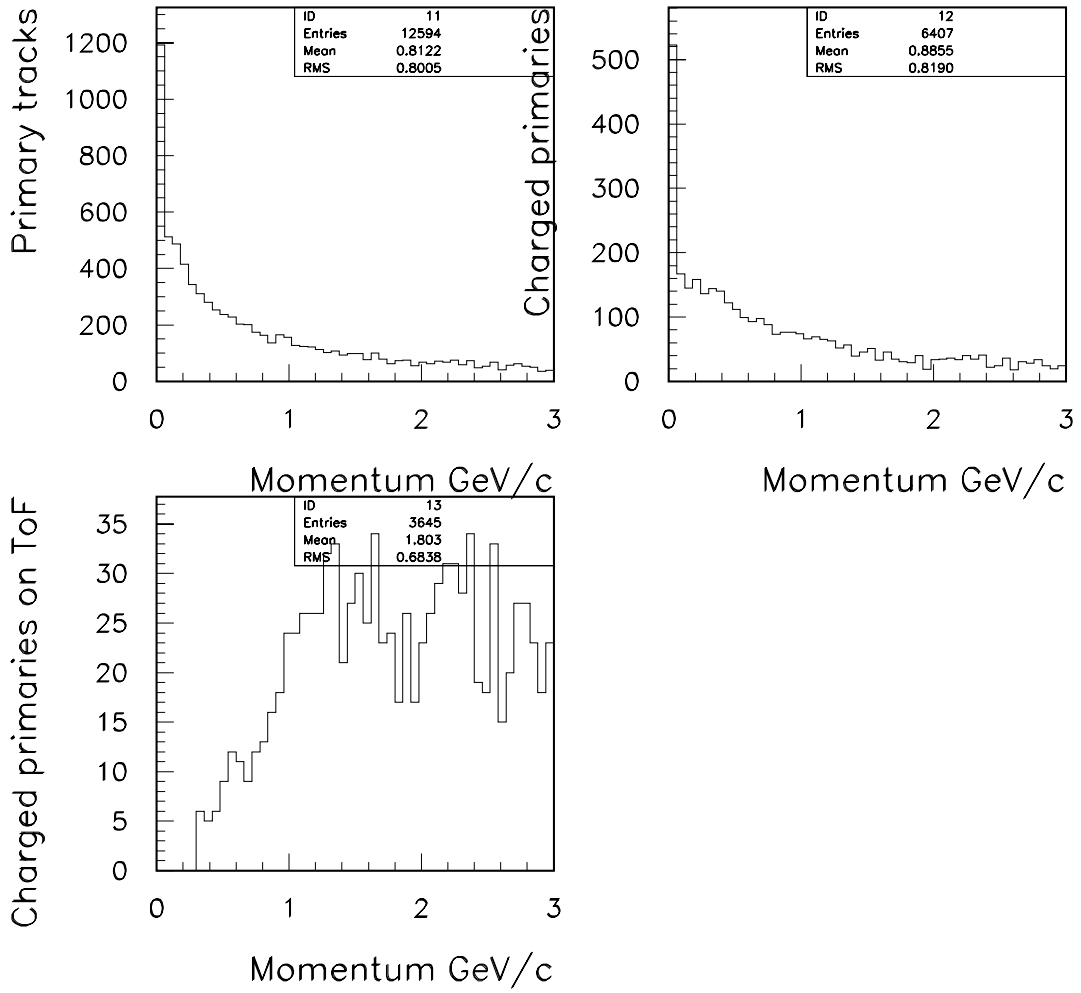

Figure 9 Figures show the momentum spectrum of all tracks, all charged tracks and all charged tracks the hit the ToF system

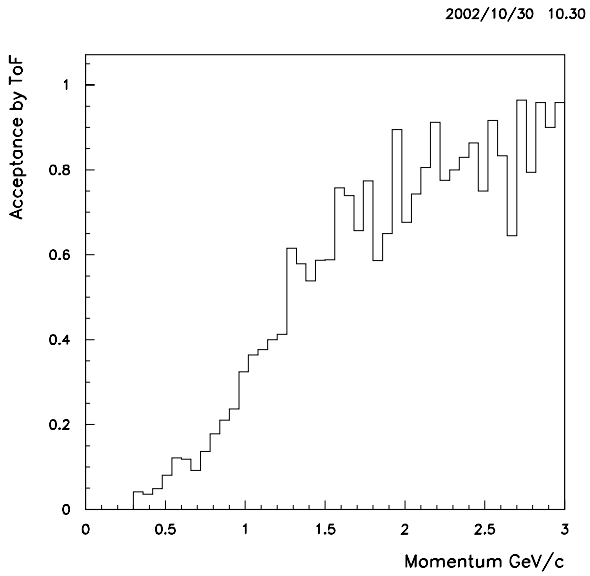

Figure 10 Figure shows the acceptance of the ToF system as a function of momentum

Testing Hypotheses

We now test the power of the ToF in differentiating between the mass hypotheses. For each particle, we compute β by the time of flight and the length of flight as given by the Geant Runge-Kutta tracker (modified to include electric fields by me; this modification also calculated the time of flight integral correctly.) Figure 11 shows the mass^2 as a function of momentum for all the tracks. No smearing is done. The three bands for the three hypotheses π,K and p are flat as a function of momentum. This indicates that Geant is doing the track integral correctly. If there were slight systematics in either the length or time of flight, this would show up as a non-flat curve in this plot. Figure 12 shows the same plot with tof resolution of 150 ps for each track. We do not yet put in momentum resolution. It is evident that the maximum error in mass occurs for the pion, for the reasons discussed previously.

We can now calculate efficiency and purity curves for each of the hypotheses. A pion is said to be identified as a Kaon, if its mass^2 fluctuates sufficiently to go over to the kaon band as shown in Figure 7. In order to calculate the purity and efficiency, we need the relative abundances of the three types of particle and we rely on Pythia to provide this to us. As we change the beam momentum and species, we should redo this calculation for each such setting, since the relative abundances can change. Figures 13 and 14 show the length of flight and the time of flight distributions of all tracks that hit the ToF. Of the total of 769 tracks under 3 GeV/c in momentum, there are 604 pions, 33 Kaons and 132 protons. The time of flight, momentum and length of flight distributions seem to be independent of particle species to first order. To estimate the efficiency/purity curves we need more Monte Carlo statistics. This we do by generating particles according to the momentum and length of flight spectrums (in HBOOK, using HRNDM1) and assigning

the relative abundances in the ratio π/K/p = 604/33/132. This approach ignores correlations between momentum and length of flight which should be small. Figure 15 shows the efficiency ε of the three particle species as a function of momentum defined as $\varepsilon = \frac{\text{Number correctly identified}}{\text{Number generated}}$ in that momentum bin. Both the pions and kaons have large enough fluctuations to cross over to each other. At a momentum of 3 GeV/c, the efficiency of observing Kaons and pions drops to ~ 77%, whereas the protons retain an efficiency of nearly 100%. Figure 16 shows the purity π of the observed species defined as $\pi = \frac{\text{Number correctly identified}}{\text{Number observed}}$ in that momentum bin. Both protons and pions maintain a purity of nearly 100% up to momenta of 3 GeV/c, where as the kaon purity is seriously affected largely as a result of the large number of pions fluctuating into the kaon bin and contaminating the kaons. Kaon purity falls to ~20% by the time one get out to 3 GeV/c. Figures 17 and 18 show the efficiency and purity curves for a ToF resolution of 100ps. Significant improvement in kaon purity is seen in the 2GeV region. The kaon purity in this region can be improved further by lowering (if possible) the threshold in the differential Cerenkov such that pions begin to radiate at ~ 2 GeV/c. It should be emphasized that these curves depend on the relative abundances of the particles being studied in the physics channel of interest.

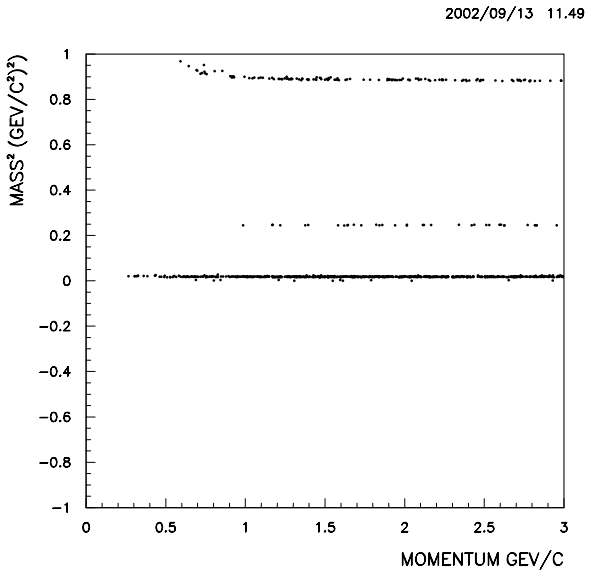

Figure 11 Mass^2 as a function of momentum with perfect time and length of flight measurements. Three bands are seen for the π, K and p hypotheses. The flatness of these curves is an indication of the correctness of the Geant tracking algorithm.

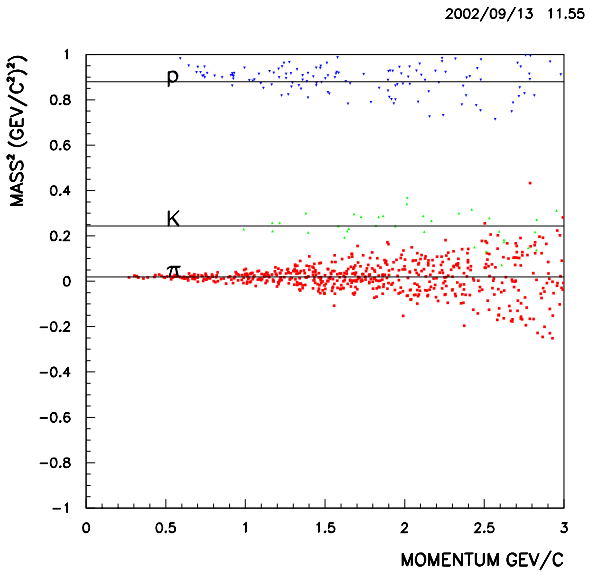

Figure 12 Same as Figure 11, but with ToF resolution of 150ps.

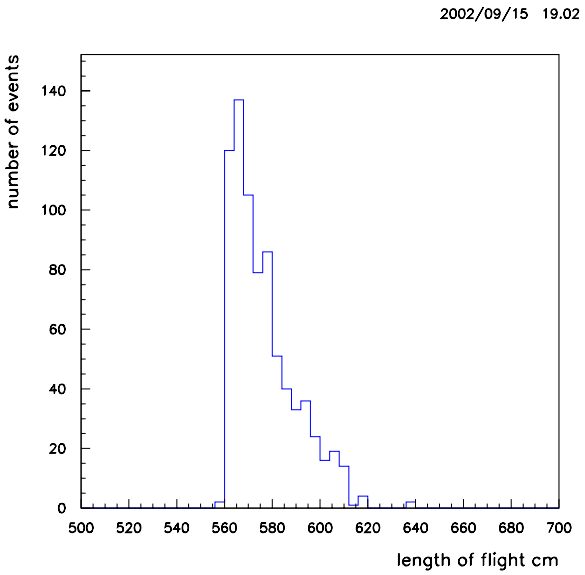

Figure 13 Distribution of length of flight of all charged tracks that hit the ToF

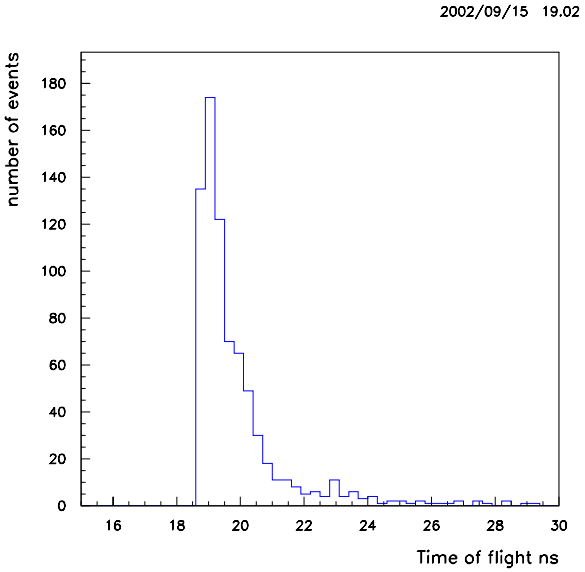

Figure 14 Distribution of time of flight of all tracks that hit the ToF

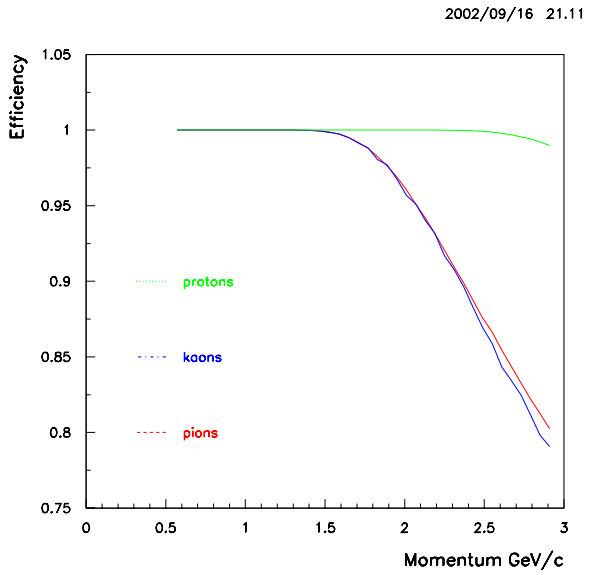

Figure 15 Efficiency curves for the three particle species as a function of momentum, ToF resolution=150ps

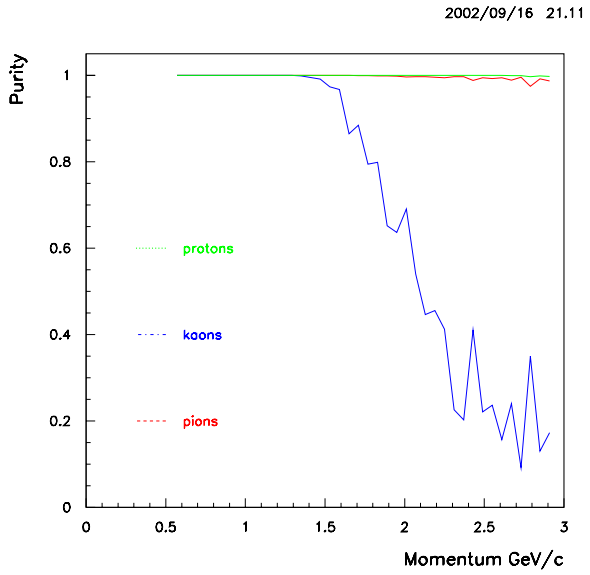

Figure 16 Purity Curves for the three particle species as function of momentum, ToF resolution=150ps

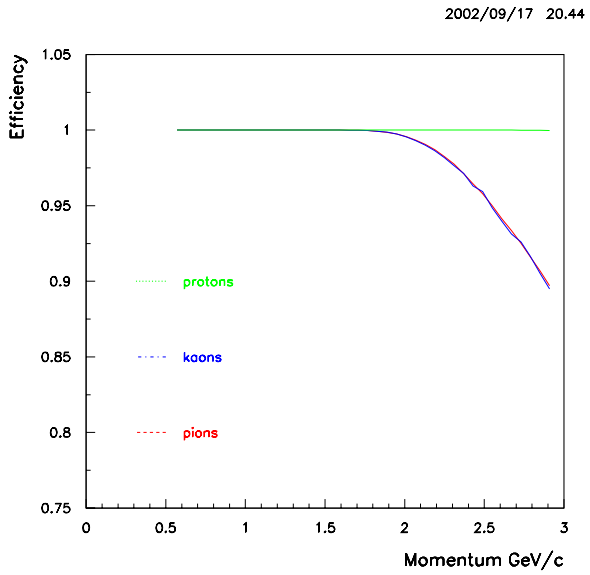

Figure 17 Efficiency curves for the three particle species as a function of momentum, ToF resolution=100ps

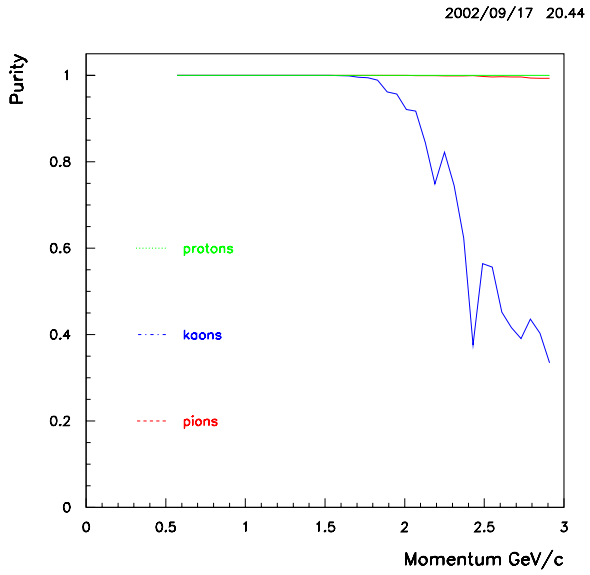

Figure 18 Purity Curves for the three particle species as function of momentum, ToF resolution=100ps

Conversion of photons

We need to study the effect of material in the detector that convert photons to produce electron positron pairs. An over abundance of such pairs will make pattern recognition in the RICH difficult, since most electrons will radiate in the RICH. Figures 19 (20) show the z co-ordinate of the vertex of origin of all(energy> 0.3GeV) the $e^{+}e^{-}$ pairs in the 1000 events under consideration. It is evident that the back of the Cerenkov box produces the largest number of pairs, followed by the TOF system The RICH mirrors and the RICH back vessel also contribute but are not significant. The pairs produced in the RICH front

occur largely outside the RICH entry window. The Cerenkov back plane in the Monte Carlo has aluminum sheets in it. This is being replaced by glass(?) in MIPP, so we expect a slightly better conversion probability in MIPP.

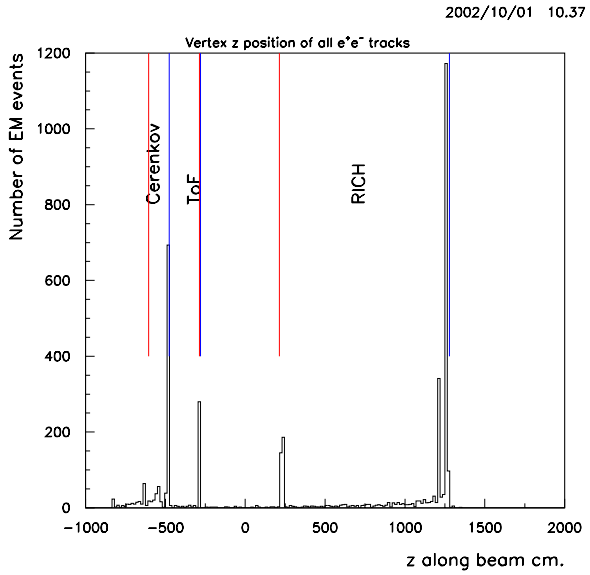

Figure 19 The vertex of origin of all e^+e^- pairs. Primary vertex is at –832.5cm. The upstream end (red) and the down stream end (blue) of the Cerenkov, ToF and RICH are shown.

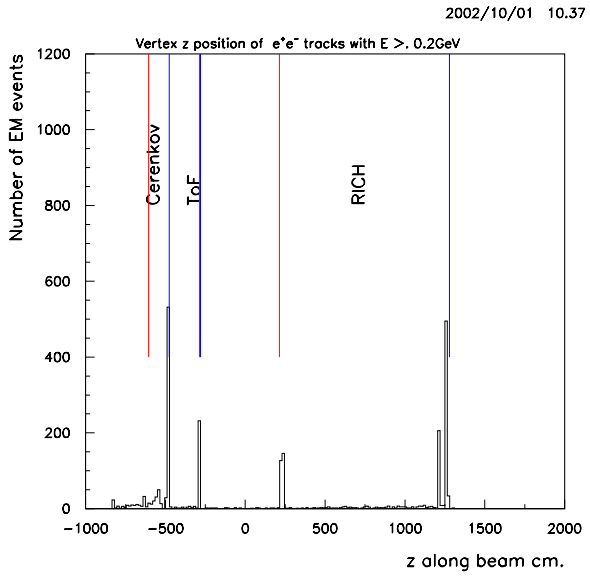

Figure 20 The vertex of origin of e^+e^- pairs with energy >0.3 GeV. Primary vertex is at –832.5cm. The upstream end (red) and the down stream end (blue) of the Cerenkov, ToF and RICH are shown.

Photon impacts on ToF

Figure 21 shows the plot of impact points (x vs y) of photons with energy > 1 GeV at the ToF. There is a concentration at the center as expected. Figure 22 shows the plot of the radius of the impact point , defined as $r = \sqrt{(x^2 + y^2)}$ of these photons.

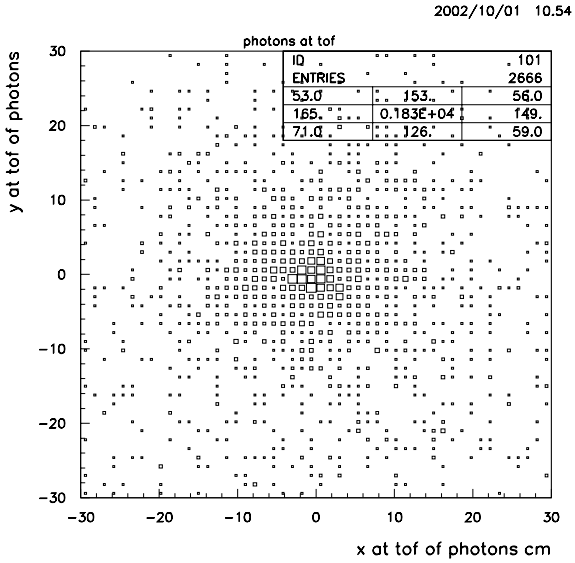

Figure 21 Impact point of photons with energy > 1 GeV at the ToF

If one were to contemplate a hole of 5 cm radius at the ToF, centered around the beam spot, we can expect to remove 444 out of the 2666 photons in the plot. This is a reduction of 16%. This is dependent on the energy of the beam, if we assume the photon transverse momentum spectrum to be independent of beam energy. If instead we make the central two counters (10 cm wide in x) to be of half the thickness, we can cut the conversion rate by 404/2666=15.4%. Figures 23 and 24 show the corresponding x and r distributions at the ToF of all charged primary hadrons with energy less than 2.5 GeV. The loss of charged hadrons by having a hole in the ToF of 5 cm radius would be 0% (=0 out of 772 hadrons)and the fraction of charged hadrons affected by having a slimmer 10 cm sliver in x would be 2.1 % (=16 out of 772 hadrons).

The main difficulty due to pair conversions is experienced in the RICH pattern recogniton in events where electrons of sufficient energy are produced that make it through ROSIE to reach the RICH. Uninteracted beam causing secondaries in either the Cerenkov or ToF is of no concern. There are 2666 photons with energy greater than 1 GeV impinging on the ToF. There are 414 electrons or positrons with energy greater than

0.5GeV with vertices starting at the ToF. This leads to a conversion probability of ~7.95%. These probabilities as well as the relative number of conversions at the Cerenkov and the time of light needs further study.

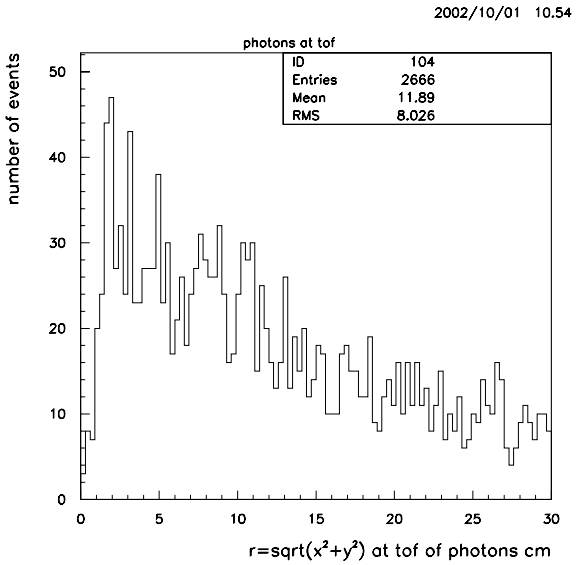

Figure 22 The radius of the impact point of photons with E>1 GeV at the ToF

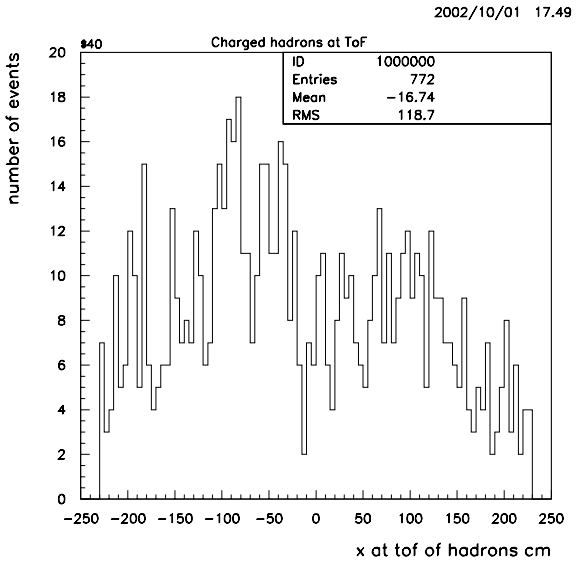

Figure 23 x distribution of primary charged hadrons with energy < 2.5 GeV at the ToF.

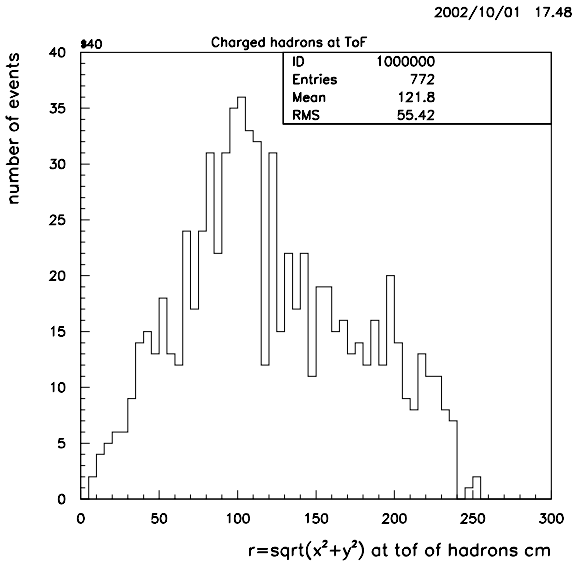

Figure 24 r distribution of primary charged hadrons with energy < 2.5 GeVat the ToF.

Electrons/Positrons entering RICH

We need to ask how many electrons (or positrons) enter RICH that originate from the ToF and where in the ToF they are produced. Figure 25 is a plot of the x y distribution at the ToF of the e+/e- tracks with energy greater than 1 GeV that enter the RICH and originate at the ToF. A Rosy field of –0.6Tesla was used for this calculation. In 1000 events there are 31 tracks that enter RICH. A full RICH pattern recognition program will have to be embarked on to see if this is a problem. However, not all these tracks are produced at the center of the ToF. So having a hole in the ToF at the beam spot will not eliminate these tracks. In contrast only 24 tracks produced at the Cerenkov enter the RICH, since the Cerenkov is further away from Rosy.

Average Hit multiplicity in ToF

Figure 26 shows the average hit multiplicity of charged tracks in the ToF counters for these tracks. Each bin in the histogram is one counter. Figure 27 shows the average hit multiplicity of charged tracks with energy < 2.5 GeV for which the ToF can provide some information. Figure 28 shows the ratio of the figures 27 and 26, which is the signal /Signal+Background in the counter, where background represents tracks with energy >2.5 GeV. It can be seen that for 100 GeV pp events, the central counters have a very low signal to background ratio.

Momentum Resolution of tracks entering ToF

From the momentum resolution study done earlier, the maximum value of $\delta p/p$ at p=3 GeV/c is 0.06% for tracks exiting after being measured by the TPC and the first wire chamber. By the time these tracks get to the ToF, they are measured even better. So momentum resolution does not add significantly to the ToF mass resolution.

Optimizing the number of counters

The counters in the center have a large number of background tracks. The (signal/signal_background) ratio for the center counters is ~0.02 where as the loss in acceptance of tracks less than 2.5 GeV by removing one counter in the middle is ~ 0.01, assuming a roughly flat distribution in Figure 27. If one were to remove the center 6counters, this would leave a 25cm gap which will cause a 6 loss in acceptance in the ToF. This would ameliorate the photon conversion problem significantly. In addition, the average charged multiplicity of tracks in counters with |x|>100cm is < 0.02, if one increases the width of the counters to 10cm for |x|>100cm, then the average multiplicity of tracks in these counters will be <0.04. The number of counters would go from 92 to 66 with this modification. If one were to remove the central 6counters, we can get by with 60counters in all. This would represent a reduction in total number of phototubes from 194 to 120 i.e a reduction of 38% in phototube costs.

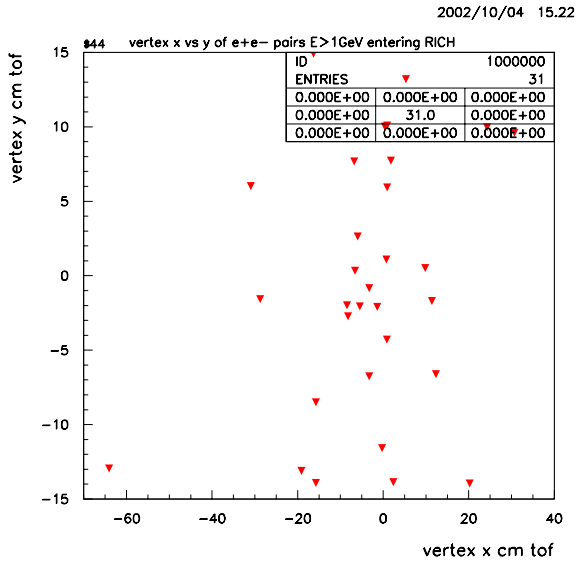

Figure 25 Vertex x y of electrons/positrons produced at the ToF that enter RICH

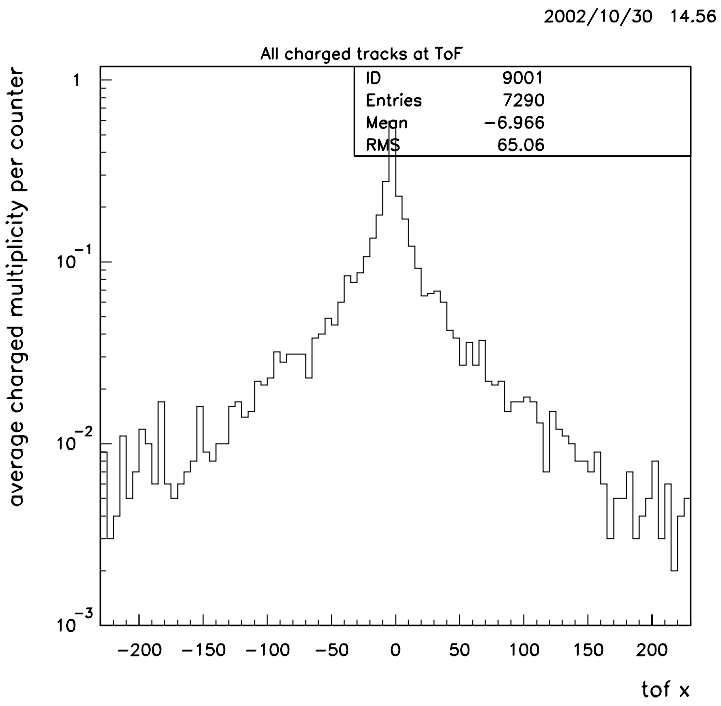

Figure 26 Averaged Charged multiplicty at ToF counter

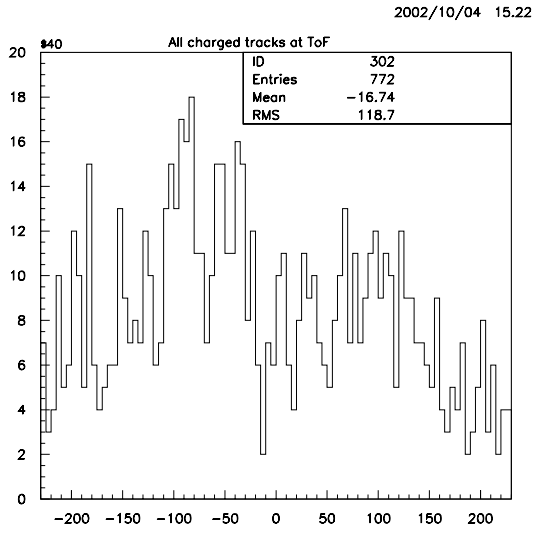

Figure 27 Averaged multiplicity of charged tracks with Energy < 2.5 GeV at ToF

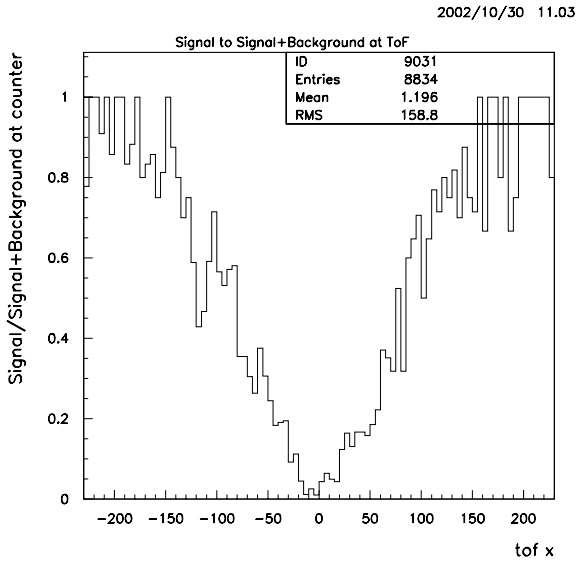

Figure 28 Signal/Signal+Background at the ToF Counter